WILL THE SOUTHERN AFRICAN WEST COAST FOG BE AFFECTED BY FUTURE CLIMATE CHANGE?

Results of an initial fog projection using a regional climate model

Andreas Haensler, Jan Cermak, Stefan Hagemann and Daniela Jacob

Summary: We present an initial study to project the long-term development of fog occurrence along the southern African west coast. For this purpose, we implemented a basic fog diagnostic scheme based on liquid water content into the regional climate model REMO. The validation of the fog diagnostic scheme is conducted using satellite-derived low cloud information as well as local station observations. The validation reveals that REMO is able to adequately represent the major fog characteristics in the region. The observed strong fog gradient from the coast to the regions further inland is correctly simulated by the model. Also, the seasonal as well as diurnal fog distribution characteristics are captured by REMO. However, some deficits still remain in the absolute amount of simulated fog days. These deficits can mainly be attributed to the coarse vertical resolution of the model as well as to the simple fog diagnostics approach chosen. Regarding the long-term development of fog, two 20-year time slice simulations for a control (1981 to 2000) and a future (2081 to 2100) period following the A1B emission scenario were conducted. The model generally projects a slight increase in the number of fog days for the coastal areas and a slight decrease for the regions located further inland. Especially the latter has the potential to exacerbate the existing water scarcity in the region.

Zusammenfassung: Nebelniederschläge spielen eine bedeutende Rolle für die Wasserversorgung der Küstenregionen des südwestlichen Afrikas. Es ist in dieser Region daher von großer Bedeutung, die zukünftige Entwicklung des Wassereintrags durch Nebelereignisse abzuschätzen. Der vorliegende Beitrag präsentiert die ersten Ergebnisse einer Langzeitsimulation des Auftretens von Nebelereignissen entlang der südwestafrikanischen Küste. Die Simulationen wurden mit dem regionalen Klimamodell REMO durchgeführt, in welches zu diesem Zweck eine Nebeldiagnostik implementiert wurde. Das Modell wurde sowohl mit Satelliten als auch mit vorhandenen Stationsdaten validiert. Generell kann REMO die vorherrschenden Muster der Nebelhäufigkeit in der Region wiedergeben. Dies trifft insbesondere auf den starken Gradienten des Nebelvorkommens von der Küste hin zu den Inlandgebieten zu. Auch der saisonale Verlauf der Nebelverteilung sowie der zugehörige Tagesgang werden zufriedenstellend vom Modell wiedergegeben. Nichtsdestotrotz treten bezüglich der absoluten Nebelhäufigkeiten deutliche Unterschiede zwischen dem Modell und den Beobachtungen zu Tage. Um eine mögliche Langzeitentwicklung des Nebelvorkommens abzuschätzen, wurden in dieser ersten Studie Nebelprojektionen für Zeitscheiben von jeweils 20 Jahren für heutiges (1981–2000) und zukünftiges (2081–2100) Klima durchgeführt. Diesen Projektionen liegt eine Treibhausgasentwicklung des A1B Szenarios zu Grunde. Die Simulationsergebnisse zeigen generell einen leichten Anstieg der Nebelhäufigkeit im Bereich der küstennahen Gebiete auf, während für Inlandregionen ein Rückgang der Nebelhäufigkeit projiziert wird. Insbesondere letzteres würde die bereits heute in der Region vorherrschende Wasserknappheit deutlich verschärfen.

Keywords: Fog modeling, regional climate model, downscaling, Namib Desert, satellite remote sensing, Meteosat Second Generation

1 Introduction

In the present study, a first attempt for a long-term projection of future changes in the occurrence of fog along the southern African west coast is described. In this region advected sea fog is a rather frequent feature (e.g. Schulze 1969; Lancaster et al. 1984) and provides a major source of moisture for several local species (e.g. Hachfeld 2000; Hamilton et al. 2003; Henschel and Seely 2008). Maximum monthly precipitation from fog can reach up to about 50 mm (Lancaster et al. 1984). The formation of sea fog in this region is linked to the relatively cold surface waters of the Benguela upwelling system. Warm air passing over these upwelling regions is cooled and reaches saturation. However, not only the occurrence of the upwelling cell matters, but also its spatial extent, which is determined by the regional wind

patterns (Shannon 1985). Olivier and Stockton (1989) postulated that a too large upwelling cell prevents the formation of fog at Lüderitz, whereas an intermediate sized upwelling cell is favorable for fog formation. This finding is linked to the fact that in 75% of all fog events at Lüderitz a coastal low was present. This coastal low is responsible for the transport of dry air masses over warm waters, where they take up moisture. These moist air masses are then transported over cold waters closer to the coast. There the air masses cool to dewpoint and fog forms. If the upwelling cell is too large, however, water uptake is reduced and therefore saturation will not be reached (Olivier and Stockton 1989). A schematic of the major upwelling cells as well as of the coastal low and the related flow scheme is included in figure 1a. It has to be noted, that the upwelling is not a constant feature as indicated in the figure but occurs in pulses (Shannon 1985).

Due to its ecological importance, fog has been regularly observed along the southern African west coast for many years. Based on observations it was shown that fog regularly extends more than 100 km inland (e.g. Lancaster et al. 1984; Hachfeld and Juergens 2000) but the number of fog days shows a remarkable gradual decrease from the coast to inland regions. Also, a distinct seasonality in the number of fog days is observed. At the coast, fog is most common in the winter (April to September) season, whereas further inland the main fog season is shifted to early summer (October to March). However, the number of available stations is limited. Therefore, Olivier (1995) established a visual analysis of satellite imagery for the detection of spatial fog extent for the year 1984. It was shown that during the observation period more than 100 fog days occurred along the coast and more than 50 fog days a year were recorded for a band reaching about 50 to 80 km inland. However, as the visual fog identification is quite cumbersome, a method to automatically detect fog is necessary when extending the observed time period. Cermak (2011) therefore recently applied an automated fog/low cloud detection algorithm to Meteosat imagery data for this region for the period 2004 to 2009. This dataset will be used in the present study for the validation of the simulated fog patterns and is described in section 3 in more detail.

Due to its frequent occurrence in a desert region otherwise very poor in precipitation, several studies have suggested the use of fog as a source of drinking water (e.g. Shanyengana et al. 2002; Olivier and de Rautenbach 2002; Olivier 2004). In the future the potential of fog for drinking water supply can be-

come even more important, as many studies report a decrease of projected future rainfall precipitation for the south-western African region (e.g. Christensen et al. 2007; MacKellar et al. 2007; Haensler et al. 2010a). However, the long-term development of fog occurrence has not been studied so far. Under this aspect, projections of long-term future developments of fog frequency would be of great value. So far, fog modeling has only been conducted for short timescales, mainly with respect to aviation and road traffic safety using one-dimensional fog forecast models (e.g. Bott and Trautmann 2002; Haeffelin et al. 2010) or 3D numerical weather prediction systems (e.g. Mueller et al. 2010). For the latter method, several simulations for specific case studies of advection fog events have been reported in the literature (e.g. Pagowski et al. 2004; Fu et al. 2006). The former study showed that the initial soil moisture conditions might have a sensitive influence on the fog simulation. However in long-term regional climate simulations the initial conditions are of less importance (Jacob and Podzun 1997). A recent study by van der Velde et al. (2010) pointed out that a high vertical resolution in the boundary layer seems to be essential for simulating the fog formation with 3D models. A comprehensive review of past achievements in fog research and fog modeling was provided by Gultepe et al. (2007).

The aim of the present study is to test the potential of the regional climate model (RCM) REMO (Jacob 2001) to project future changes in fog frequency over the region. We therefore implemented a fog diagnostic scheme into the model. REMO has already been applied for hindcast (Haensler et al. 2010b) as well as transient climate change (Haensler et al. 2010a; c) simulations over the southern African region. In these studies it has been shown that the model is well suited to simulate the region's climate characteristics. Especially due to the very high horizontal resolution of the simulations, region-specific climate features have been shown to be better simulated by REMO than by reanalysis data (Haensler et al. 2010b).

In section two, the model and the fog diagnostics are described. In section 3 the available fog datasets, as well as the methods used to validate the model and to assess potential future changes in the fog occurrence are presented. Section 4 shows the results of model validation and of the future fog projections. Finally, section 5 provides a discussion of the findings of the validation and climate change sections. The paper ends with a short conclusions section.

2 Model description and simulation setup

The simulations are conducted with the three-dimensional hydrostatic atmospheric circulation model REMO (REgional MOdel) (JACOB and PODZUN 1997; JACOB 2001) in its 2008 version. This version was already tested and used over the southern African region in an previous study (HAENSLER et al. 2010a). The model is based on the "Europamodell", the former numerical weather prediction model of the German Weather Service (MAJEWSKI 1991). In its original version the physical parameterizations of REMO were based on those of the global climate model ECHAM4 (ROECKNER et al. 1996). The prognostic variables of REMO are surface pressure, horizontal wind components, temperature, specific humidity and cloud water. With respect to the fog simulation especially the calculation of the cloud water of large-scale (stratiform) clouds in REMO is of interest. For the stratiform clouds this calculation is based on the approach following SUNDQVIST (1978), and was taken from the ECHAM4 global climate model (ROECKNER et al. 1996). The budget equation for cloud water is calculated including the processes of evaporation of cloud water as well as condensation of water vapor. Also the advective and sub-grid scale transports of cloud water are incorporated in the equation. The vertical turbulent transfer of momentum, heat and water vapor fluxes are based on the Monin-Obukhov similarity theory for the surface layer and on the eddy diffusivity approach above the surface layer (LOUIS 1979).

The horizontal resolution for the simulations described here is 18x18 km. In the vertical direction the model was run with 20 levels, with the lowest model level approximately 30 m high. The model was integrated for a hindcast simulation for the period from 2001 to 2007 and for two 20-year simulations (Control: 1981–2000; Scenario: 2081–2100) as an initial study to assess potential changes in fog occurrence. The lateral boundary conditions for the simulations are taken from ERA40 reanalysis (UPPALA et al. 2005) and operational analysis data of the European Centre for Medium-Range Weather Forecasts (ECMWF) for the hindcast and from the coupled atmosphere ocean general circulation model ECHAM5/MPIOM (ROECKNER et al. 2003; JUNGCLAUS et al. 2006) IPCC A1B projections for the climate change simulations. To reach the final 18x18 km resolution the so-called double nesting setup was applied. In this setup the original boundary forcing is first downscaled to an intermediate resolution REMO simulation (50x50 km) and the output of this simulation is then used to force the high-resolution simulation. An overview of the simulation setup including the double nesting setup is given in figure 1b.

2.1 Fog diagnostics

Fog is generally defined via the visibility (VIS) and occurs if VIS is lower than 1000 m (WMO 1992). In REMO, VIS is not an output variable. To identify
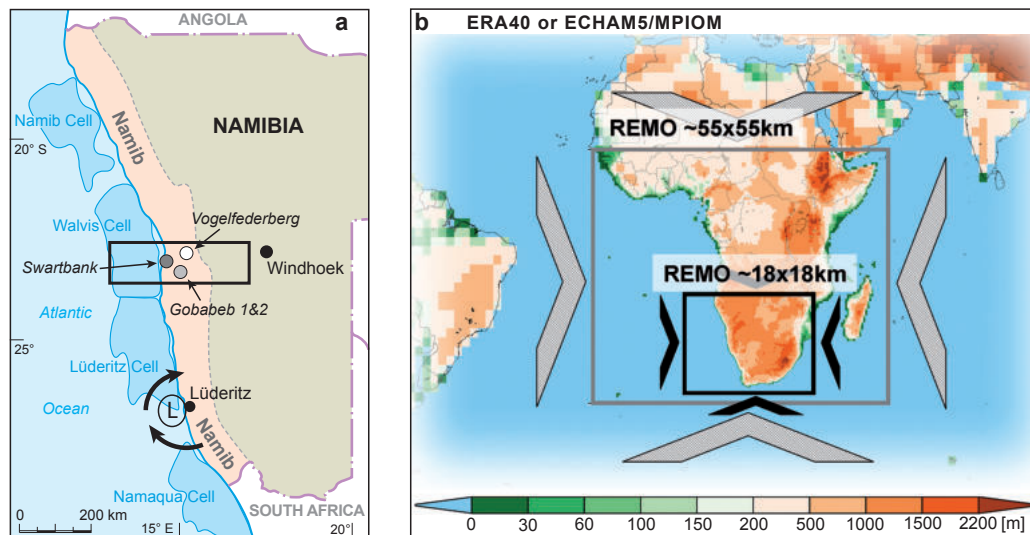

Fig. 1: (a) Location of the four available stations with fog observations The panel also depicts the main Benguela upwelling cells after PICKFORD and SENUT (1999) and a schematic of the coastal low and its related flow fields after OLIVIER and STOCKTON (1989). The black rectangle indicates the location of the east-west transect described in figure 3. (b) Sketch of the double nesting setup and extent of the respective REMO domains indicated as grey (~55 x 55 km) and black (~18 x 18 km) boxes

fog events we therefore implemented the visibility parameterization after KUNKEL (1984) into REMO. The diagnostics is a function of the liquid water content (LWC) and follows

$$VIS = -\frac{\ln(0.02)}{144.7(LWC \times \rho)^{0.88}} \qquad (1)$$

with ρ representing air density. Fog is diagnosed only in the lowermost model level but at each model time step. This diagnostic is frequently used in modeling studies (e.g. TEIXEIRA 1999) but due to its simplicity it seems to have some disadvantages. GULTELPE et al. (2006) showed that the simulation results can be significantly improved if the droplet number concentration Nd is taken into consideration. However as Nd is still a preset parameter in the current REMO version the proposed relation could not be used in the present study.

The output interval of the fog simulation was set to one hour, even though fog was diagnosed on a 90 seconds time step. Hence the resulting model output is the fraction of an hour, on which the model simulates fog. In order to compare the simulated fog data to observations on a daily basis (and to not include fog events only occurring on a single model timestep into the analysis) a threshold had to be defined, to distinguish between fog and fog-free days. This threshold for a fog day was defined in a way that at least for 75% of a single hour a day the model has to simulate fog conditions. This definition translates to a minimum of 45 minutes of fog a day in order to be counted as a fog day, which allows identifying both short-term fog events (less than one hour) and long-term fog events.

3 Data and methods

3.1 Available observations

For the validation of the simulated fog occurrence, a fog/low cloud product derived from Meteosat satellite imagery at a horizontal resolution of 3 km is used (CERMAK 2011). In contrast to previous geostationary satellite systems, the Spinning-Enhanced Visible and Infrared Imager (SEVIRI) aboard the newest Meteosat satellites features high spatial, temporal and spectral resolutions, which makes it suitable to be used for cloud type discrimination (CERMAK et al. 2008). Areas covered by fog and low clouds can be identified on the basis of spectral tests in the visible and infrared regions, informed by radiative transfer computations incorporating the principles discussed in CERMAK and BENDIX (2008). Originally, this product was only available for Europe, where it could be tested against station observations.

Recently CERMAK (2011) transferred the procedure to the southern African region to develop a new product for the identification of fog and low clouds along the south-western African coast for the period from 2004 to 2009. Based on information obtained in radiative transfer modeling, a set of thresholds was found in six infrared and visible-range channels that allows for the robust delineation of fog and low clouds in the region. These tests are applied sequentially and lead to the subsequent exclusion of various surfaces other than fog and low clouds. Visual inspection as well as a numerical validation study confirmed the absence of artifacts, especially along the coast line. As no station data was available for this period, the validation of the fog/cloud product had to be based on Cloud-Aerosol Lidar with Orthogonal Polarisation (CALIOP) data. Generally, the new product was found to be reliable (hit rate above 95%). However, fog and low clouds hidden underneath higher cloud layers cannot be identified. For the south-western African region a data set indicating fog/low cloud presence and absence was compiled covering two time periods each day (0700 and 1400 UTC). A full description of the technique and its validation, as well as a climatological interpretation of the product is given in CERMAK (2011).

In addition to the satellite data, manually recorded daily station data were available for four stations located in the central Namib Desert (see Fig. 1a and Tab. 1). These data are based on instantaneous 8 am (local time) visual observations as well as cumulative fog measurements (via passive fog samplers) at the respective weather stations. At one of these stations also hourly data derived from a passive fog sampler was available for a limited time period. However, apart from the hourly time series, these datasets are affected by significant data gaps. Moreover, they are based on different measurement techniques and also do not cover the same period (see Tab. 1). Therefore these data are only considered as an additional data source to assess the quality of the satellite and model data, rather than a real validation dataset. The shortcomings in the observed data are also the reason for evaluating only the occurrence of fog events but not the actual amount of fog water input.

Tab. 1: Locations and sampling periods of the four stations in the central Namib with fog observations

	Latitude	Longitude	Sampling Period
Swartbank	23.2° S	14.5° E	1970–1982
Gobabeb 1	23.4° S	15.0° E	1966–1995
			2000–2002**
Gobabeb 2	23.5° S	15.0° E	1981–1995
Vogelfederberg	23.0° S	15.3° E	1979–1992
Satellite	–	–	2004–2009

(** hourly readings)

3.2 Validation of the model

To validate the implemented fog diagnostics, we applied the REMO model for the period from January 2001 to August 2008 using ERA40 and operational analysis data as lateral boundaries. However, for the validation, only the 4 year overlap period with the satellite data from 2004 to 2007 is regarded.

Even though the time period of model/satellite and station data do not match, we still considered the station data as an additional data source, mainly for assessing the relative seasonal and diurnal cycles. However, as a regional model is not intended to represent the climatic features at each single gridbox, the standard procedure when comparing model data to station data is to average the model output over a larger number of model grid boxes centred around the station. In order to compare the number of fog days received by the satellite and the model directly to the station observations, we therefore used an inverse distance-weighted method to compute the number of fog days for the gridded satellite and model data at each station location.

Not only the simulation of the annual mean fog occurrence was validated at each of the station locations but also the simulation of its seasonal evolution was considered. In order to better compare the simulated and observed seasonalities (even though the absolute number of fog days differs) all data have been normalized to the respective climatological maximum monthly fog occurrence at the respective stations. Furthermore, at one station this method could also be transferred to the evaluation of the simulation of diurnal fog characteristics.

3.3 Quantifying changes in the future fog extent

For the assessment of future changes in the fog occurrence along the southern African west coast we forced the regional climate model REMO with the output of the coupled global atmosphere-ocean model ECHAM5/MPIOM. We simulated two 20-year time-slices for the periods 1981–2000 (control) and for 2081–2100 (scenario) for this initial study. For the future period the greenhouse gas concentrations followed the concentration path of the SRES A1B emission scenario (Nakicenovic et al. 2000), which represents an intermediate emission pathway. For this scenario a transient climate change projection has already been conducted with REMO, using the same model setup, however without the fog diagnostics. In the current study the projected climate change signals under this emission scenario with respect to temperature, precipitation and circulation are only briefly mentioned in section 4.2. A detailed discussion of the findings of the transient climate change projections can be found in Haensler et al. (2010a), Haensler et al. (2010c) and Haensler et al. (2011).

4   Results

4.1 Model validation

The mean number of simulated fog days is compared to the satellite observations on an annual as well as on a seasonal (Summer: October to March; Winter: April to September) basis (Fig. 2). Generally, the satellite data show a strong negative gradient in fog occurrence from the coast to locations further inland. At the coast the maximum number of fog days is around 160 days per year. According to the satellite product, up to about 200 km inland an average of at least 5 fog days per year is observed around the central Namib. Seasonally, the satellite shows more fog days for the summer season. A comparison with the model reveals that REMO is able to simulate the general seasonal and spatial patterns of fog, with more fog at the coast and less fog further inland. However, the model seems to overestimate the fog occurrence at the coast and over the ocean and underestimate the number of fog days further inland. This seems
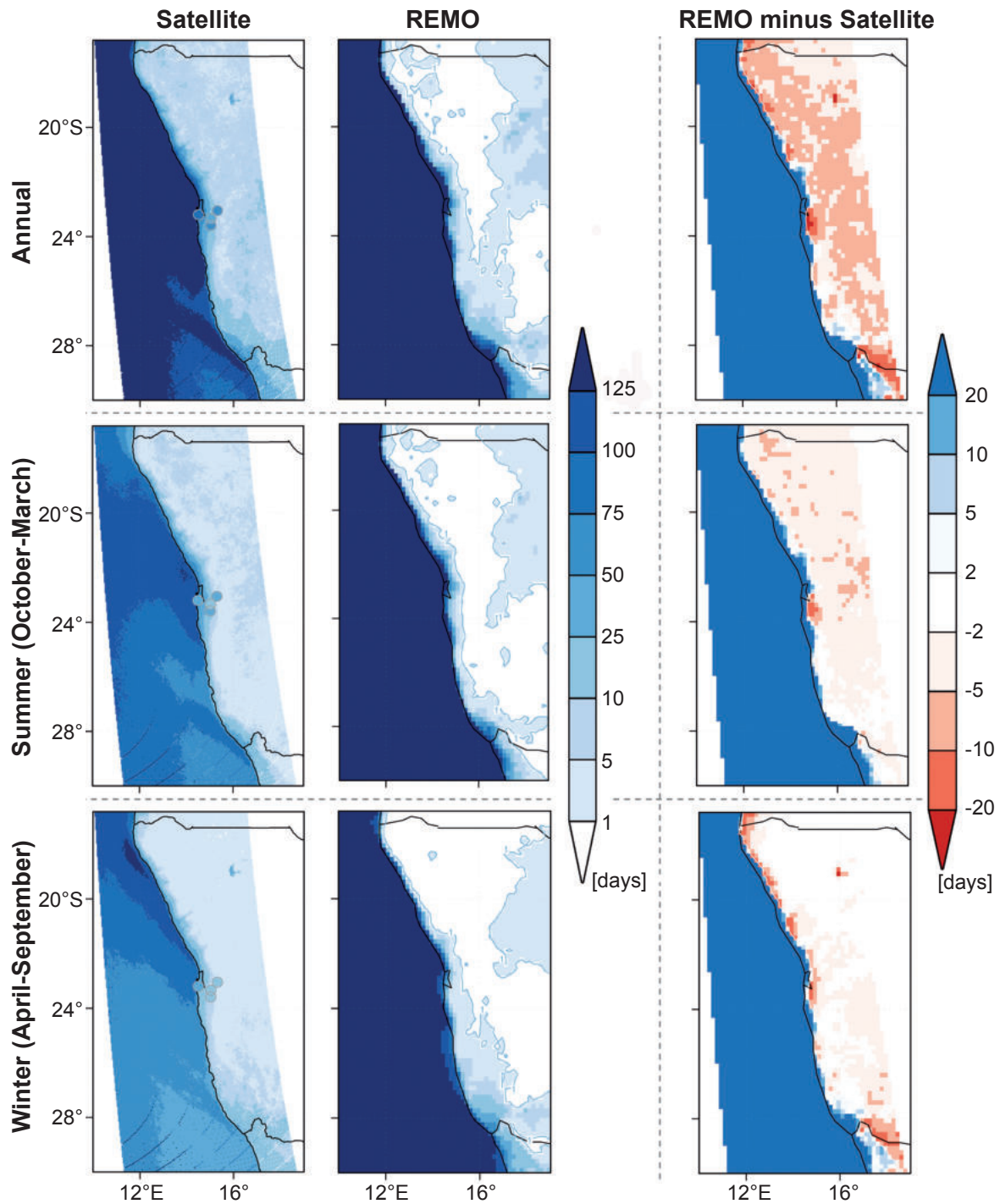
Fig. 2: Mean number of fog days per year (upper row) and for the summer (central row) and winter (bottom row) seasons as observed (left column) and simulated by REMO (central column) for the period from 2004 to 2007. Additionally the observed fog days at each station, represented by coloured circles, are included in the left panels. However the time period of the data differs from the satellite and model (see Tab. 1). The absolute differences between simulated and observed fog occurrence for the respective seasons is displayed in the right-hand panel. Note that the 3 km satellite data was remapped (using a first-order conservative remapping method) to the 18 km REMO grid for direct comparison

to be the case for both, the summer and winter seasons. Figure 2 depicts also the number of fog days recorded at the four stations. Here a much lower gradient from the coast towards the interior is visible compared to the model but also to the satellite data. This can also be seen in figure 3, which shows the mean number of fog days along a west-east transect (13°E to 17°E; 22.8°S to 23.8°S) as simulated with REMO and observed by the satellite and the stations. The strong overestimation in the number of fog days over the ocean areas is visible. In the transition zone a strong decrease in the number of fog days occurs. REMO overestimates the fog frequency up to ~25 km inland, while further inland the model slightly underestimates the number of fog days.

In comparison to the stations, both, the satellite data as well as the model show a stronger gradient in the mean number of fog days per year from the station closest to the coast (Swartbank) to the inland stations (Gobabeb and Vogelfedersberg) than those recorded at the station (Tab. 2). Especially the pronounced difference of the satellite and station data has to be noted. This difference can partly be assigned to the interpolation of the gridbox average to the point location. But the remaining discrepancies still show that also the observations suffer from a particular degree of uncertainty, which has to be kept in mind while evaluating the model re-

sults. Finally, the periods covered by each data set differ and no more than this general agreement on patterns was expected. The observed and simulated mean annual cycles for all stations are depicted in figure 4. Generally for all stations the satellite and the model show a more pronounced seasonality than the stations. This is most probably related to the fact that the station data suffer from frequent data gaps, which are not uniformly distributed within the year. However, the position of the peak is still comparable to the one of the satellite data. For the Swartbank and Vogelfederberg the mean seasonal cycle as observed by the satellite and simulated by REMO agree rather well, but REMO shows the peak fog occurrence one month earlier at Vogelfederberg and slightly later at Swartbank than observed. For the two Gobabeb Stations, the model seems to miss the secondary fog maximum in early summer which is visible in the satellite data.

At the Gobabeb Logger Station also hourly data are available. Therefore, the diurnal cycle of fog occurrence can be analyzed as well. According to the station data the maximum of fog occurrence is around 0600 UTC (Fig. 5), which fits rather well to the timing discussed in the literature (e.g. SCHULZE 1969). During daytime almost no fog occurrence is observed. REMO reproduces the observed diurnal cycle almost perfectly showing only a slight delay in
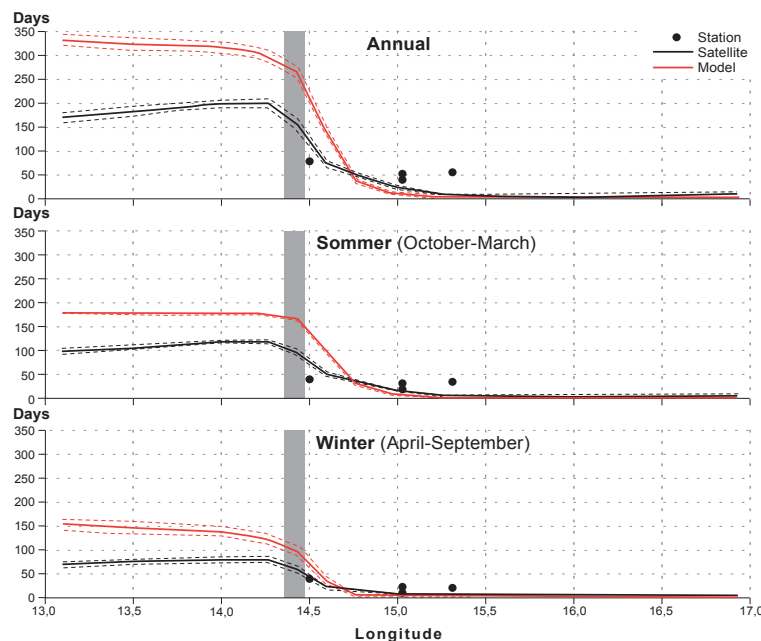

Fig. 3: Mean number of fog days per year (upper panel) and for the summer (central panel) and winter (bottom panel) as meridional mean along a west-east transect indicated as in figure 1a. The observed fog days are indicated by the black line (Satellite) and grey dots (Stations): simulated fog days by REMO are depicted in red. The satellite observations and the model cover the period from 2004 to 2007, the recording period of the stations differ (see Tab. 1). The range in the data is defined by the standard deviation. The grey shaded area represents the sea-land transition zone

Tab. 2: Summary of the annual fog statistics for the four stations as observed and simulated by REMO. Note that the data represent different time periods (see Tab. 1 and Fig. 2)

[days]	Station				Satellite				Model			
	Mean	Min	Max	SDev	Mean	Min	Max	SDev	Mean	Min	Max	SDev
Swartbank	80	62	104	13	100	82	120	14	163	152	180	10
Gobabeb 1	41	14	64	12	22	19	27	3	15	14	16	1
Gobabeb 2	55	20	73	12	28	20	33	5	11	9	15	2
Vogelfederberg	57	15	80	18	7	4	12	3	4	3	5	1

the fog maximum and a slightly shorter period of general fog occurrence than observed. Whereas the station data already records fog before midnight, the model only shows fog after midnight. Also the satellite seems to have the maximum in the morning, however, with only two samples a day a robust analysis cannot be made.

4.2 Scenario of future fog extent

The greater Namib Desert region is projected to undergo a significant warming in all seasons under the chosen emission scenario until the end of this century. The mean annual warming is projected to be in the order of about 2°C in the coastal areas to more than 4 °C further inland (Fig. 6, upper panels). However even though in the mean state a general warming is projected to occur, the diurnal temperature range seems to be only marginally affected by this change, showing a slight decrease in the future diurnal temperature range (Fig. 6, lower panels). Future rainfall amount is projected to be significantly reduced to about 50% of today's rainfall amount

(not shown), however due to the arid conditions in the region the absolute rainfall changes are rather small. Regarding the near surface circulation fields, the large scale circulation patterns slightly change (e.g. HAENSLER et al. 2011), however the thermally induced land-sea breeze and plain-mountain circulation do not seem to be strongly affected by future climate change.

However, as already mentioned above, fog water input seems to be more important in this region than rainfall. In the subsequent section, therefore the projected changes in fog occurrence under this emission scenario are presented. In figure 7, the simulated mean number of fog days per year and for the two seasons are presented for the control and scenario simulations. Generally REMO projects a slight increase of the number of fog days over the ocean and along the coastal land areas. Further inland however, a decrease in the number of fog days is projected, leading to a stronger negative gradient from the coast inland. This change pattern seems to be consistent throughout the year, as there is not much difference between the summer and winter situations. At the four station locations, the situation
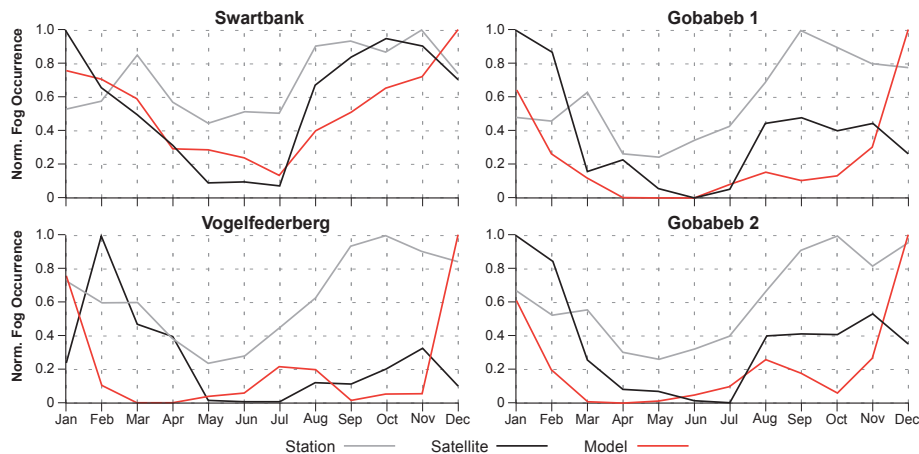

Fig. 4: Observed and simulated mean seasonal fog distribution for the four stations in the central Namib. Note that each data series was normalized to its respective maximum value. Furthermore, the data represent different time periods (see Tab. 1 and Fig. 2)
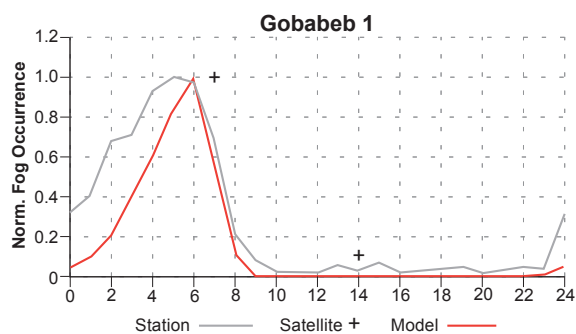
Fig. 5: Observed and simulated mean diurnal fog distribution for the Gobabeb 1 station. Note that each data series was normalized to its respective maximum value. Furthermore, the data represent different time periods (see Tab. 1 and Fig. 2)

seen in figure 6 is also represented (Tab. 3). Whereas close to the coast (Swartbank) fog occurrence is projected to slightly increase (~10%), the model results at the location of the inland stations show a decrease from about 25% (Gobabeb) to almost 40% (Vogelfederberg). The calculated decrease in the number of fog days at these three stations is limited to the main fog season during late summer, whereas the simulated secondary maximum during the winter season is slightly shifted towards early winter. The projected increase at the Swartbank station is limited to the winter season (Fig. 8). Both change patterns lead to a reduced seasonality in the projected future fog patterns. As expected no change is visible in the diurnal cycle at all four stations (not shown), since the dissipation of fog in the early morning is mainly linked to thermal processes connected to the diurnal temperature cycle. Even if the absolute temperature is projected to increase in the future (see HAENSLER et al. 2011) the diurnal temperature range is simulated to only slightly increase (~0.5K) in the future for this region. Therefore, the cooling during night time still is sufficient to maintain the presence of advected fog. As also the timing of the temperature minimum is not projected to change in the future, also the onset of the fog formation seems to be rather constant.

5 Discussion

In this paper we present a first attempt of a long-term fog projection using a regional climate model. The simulated fog occurrence shows patterns similar to those observed, with a remarkable west-east gradient in the fog occurrence from the coast to the interior. But still, there are some remarkable deviations between model and satellite observations. Especially the inland penetration of fog seems to be underestimated by the model. However, a lack in inland moisture transport simulated by the model seems not to be the cause for this deficit, as the regional circulation characteristics (HAENSLER et al. 2010b) as well as the local, thermally induced wind fields (not shown) are well reproduced by REMO. Also the seasonality and the diurnal cycle of the fog occurrence fits rather well with observations giving a further indication that the circulation patterns are captured by REMO. Hence, the deficit in inland fog simulation can more likely be assigned to the coarse model resolution and the very simple fog diagnostics that were implemented. Especially the vertical extent of the lowest model level has to be assessed critically (MASBOU 2010, pers. comm.; TARDIF 2007; VAN DER VELDE et al. 2010) and should be reduced remarkably in future applications. However as a change in the vertical resolution requires a comprehensive validation of the model itself, we decided to use the already validated model for this initial study. Other reasons for disagreements could be errors in the satellite data set mainly connected to the inability to identify fog, if high-level clouds are present. It further has to be mentioned that discrepancies in the observations and the model data could also arise from the fact, that in the model only fog in the lowest model layer is diagnosed, whereas in the satellite observations also near surface stratus might be detected. Also the internal variability of the model could be a reason as the time period for which satellite data is available is rather short. A major source of uncertainty is also the threshold set to define a fog day in the REMO model. While it has no influence on the simulated

Tab. 3: Summary of the annual fog statistics for the four stations as simulated by REMO for the control (1981–2000) and scenario (2081–2100) periods

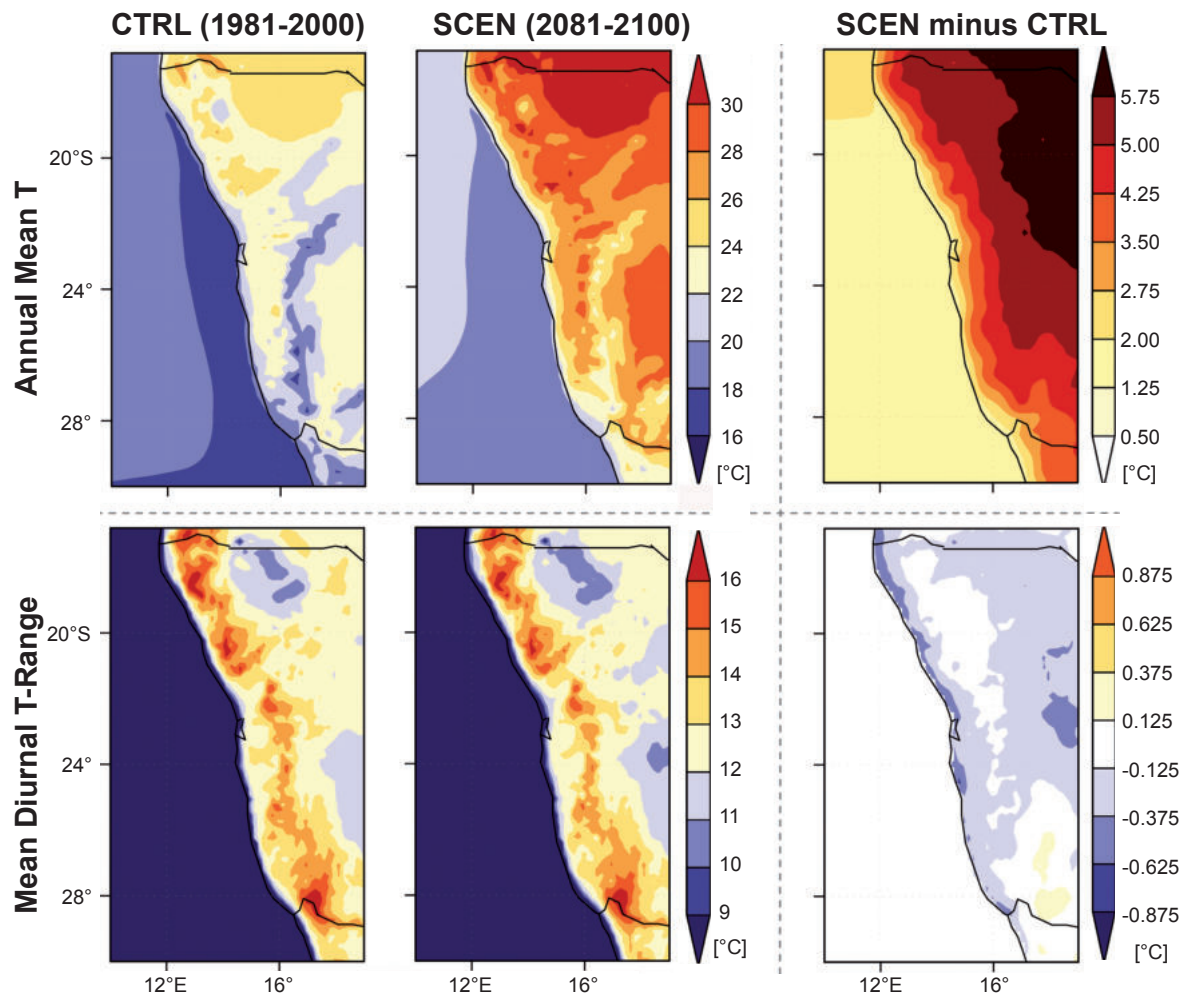| [days] and [%]	Ctrl (1981–2000)				Scen (2081–2100)				% Change	
	Mean	Min	Max	SDev	Mean	Min	Max	SDev	Mean	SDev
Swartbank	153	129	171	11	167	148	206	13	10	16
Gobabeb 1	21	10	40	7	17	6	32	7	-23	-4
Gobabeb 2	20	9	35	6	14	5	29	7	-30	6
Vogelfederberg	11	5	25	5	7	2	20	4	-39	-12

Fig. 6: Simulated annual mean temperature over the control period (1981–2000; upper left) and the projected mean changes for the scenario period (2081–2100; upper right). The lower panels show the simulated annual mean diurnal temperature range over the control (left) and scenario (right) period

fog seasonality it definitely has an impact on the absolute number of fog days. Finally the different horizontal resolutions of the satellite data and the model have to be mentioned. Thus, no more than the general agreement of patterns between model and satellite could be expected. This general agreement is therefore taken as an indication of the satisfactory representation of fog conditions by the model.

In general, however, the applicability of the simple fog diagnostic based only on the LWC has to be critically reexamined. Previous work by GULTEPE et al. (2006) shows that the error can be as high as 50%. In a recent study by SHI et al. (2010) it could be shown that the model skill to forecast specific fog events significantly increases when including the Nd into the analysis. However these findings refer to fog forecasting studies, where the timing and extent of individual fog events matter. In our approach however, we are mainly interested in the long-term changes and not in the simulation of fog events. Therefore the error is likely to be smaller. Another worthwhile approach for fog simulations with a horizontal resolution in the range of about 20km could be to use a multivariable-based fog diagnostics as proposed in a recent paper by ZHOU and DU (2010). They defined fog based on a decision cascade considering first the LWC, then the vertical cloud extent and finally 10m wind speed and relative humidity. The application of these four criteria significantly improved fog forecasting, especially wind speed and relative humidity proved to be important factors to consider. However, one has to keep in mind that the event-based verification of the decision chain, as usually performed for numerical weather forecast
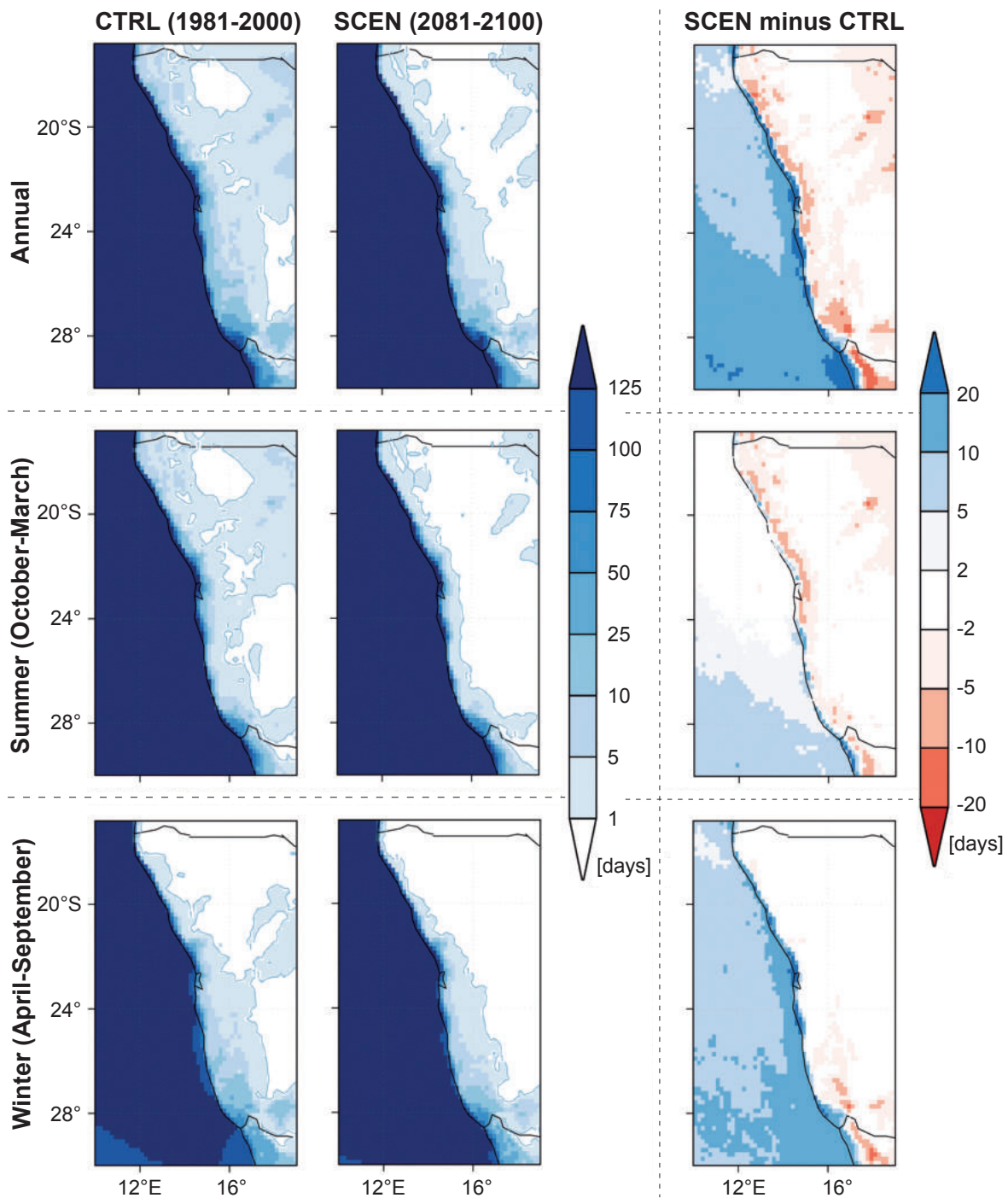
Fig. 7: Mean number of fog days per year (upper row) and the summer (central row) and winter (bottom row) seasons as simulated by REMO for the control (1981–2000; left column, 'CTRL') and the scenario (2081–2100; central column, 'SCEN') periods. The absolute differences between control and scenario fog occurrence for the respective seasons are displayed in the right-hand panel

models, cannot be applied to an RCM. Therefore, a multivariable approach might also enhance the uncertainty involved in the diagnostic process.

The presented scenario simulation gives a first indication of how reliable fog occurrence will be in the future. Generally, a decrease in the number of fog
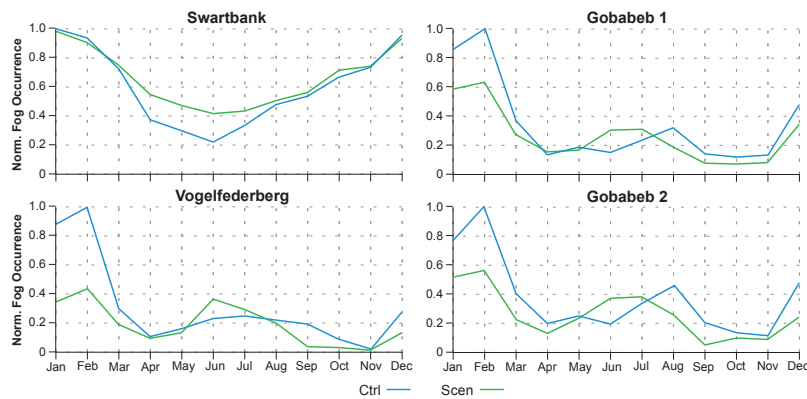
Fig. 8: Simulated mean seasonal fog distribution for the four stations in the central Namib for the control (1981–2000) and scenario (2081–2100) periods. Note that the data series are normalized to the climatological maximum value of the control period

days is projected for the inland fog leading even to the disappearance of fog in many locations. Less fog days per year will most likely lead to an overall decrease in fog water input. In connection with the projected rainfall decrease mentioned before (e.g. MacKellar et al. 2007; Haensler et al. 2010a), the regional water availability is likely to be substantially reduced in the future. The projected bipolar pattern in the change of future fog occurrence can mainly be related to the projected changes in the temperature. As there seems not to be a general change in the regional-scale circulation in the chosen scenario (even though it is largely influenced by thermal properties) a possible explanation for the reverse change in the fog occurrence might be related to changes in the thermal characteristics of the atmosphere. While the general warming over the ocean (see Fig. 6) would favor an increased moisture load at the coastal areas, the strong warming over land might favor a faster fog dissipation.

However it has to be kept in mind that for the assessment of future fog extent only 20 year time slice experiments were conducted. Therefore, the projected changes serve rather as a indication for what the future could be, than as absolute number. For a more robust projection, a longer time period needs to be assessed and more scenario simulations (also including more models) should be conducted.

It also has to be noted that due to the change of the forcing from the ERA40 re-analysis data (used on the validation simulation) to the ECHAM5/MPIOM data (used for the control and scenario simulations) a difference in the simulated fog days for present-day climate conditions appears. However, due to the fact that the deficits in the validation simulation (Section 3) are reduced in the control simulation (see Tab. 2 and 3), the application of the model for a scenario simulation seems to be justified.

Finally, the feedback of future changes in the circulation characteristics onto the regions ocean circulation should also be considered in future projections (e.g. Haensler et al. 2010c). The importance of the Benguela Upwelling system for fog formation along the southern African west coast was shown by Olivier and Stockton (1989). In the current simulation, ocean characteristics are taken from the coupled ECHAM5/MPIOM model. However, due to the coarse horizontal resolution of a GCM the individual upwelling cells cannot be resolved in the required degree of detail. Therefore, a fully coupled regional atmosphere-ocean model, such as already in place for the Mediterranean region (Elizalde 2010, pers. comm.), could provide very valuable information.

6 Concluding remarks

We presented an initial study to assess whether future climate change might influence the occurrence of fog along the southern African west coast. We found that the regional climate model REMO with a basic fog diagnostics scheme can realistically represent the major fog patterns over the region. For the future, this initial study projects an increase of fog along the coast and a decrease further inland. Keeping in mind the uncertainty of the projections, we still think that along the coast fog can act as a supplementary drinking water source for local communities in the future. However, to provide a more robust data base for regional stakeholders and decision makers, more scenarios (including multi-model ensemble simulations) have to be conducted for the region covering a much longer time period.

Acknowledgements

References

BOTT, A. and TRAUTMANN, T. (2002): PAFOG – a new efficient forecast model of radiation fog and low-level stratiform clouds. In: Atmospheric Research 64 (1-4), 191–203. DOI: 10.1016/S0169-8095(02)00091-1

CERMAK, J. (2011): Low clouds and fog along the south-western African coast – satellite based retrieval and spatial patterns. In: Atmospheric Research. DOI: 10.1016/j.atmosres.2011.02.012.

CERMAK, J. and BENDIX, J. (2008): A novel approach to fog/low stratus detection using Meteosat 8 data. In: Atmospheric Research 87 (3-4), 279–292. DOI: 10.1016/j.atmosres.2007.11.009

CERMAK J.; BENDIX J. and DOBBERMANN M. (2008): FMet – An integrated framework for Meteosat data processing for operational scientific applications. In: Computers and Geosciences 34 (11), 1638–1644.

CHRISTENSEN, J.; HEWITSON, B.; BUSUIOC, A.; CHEN, A.; GAO, X.; HELD, I.; JONES, R.; KOLLI, R.; KWON, W.; LAPRISE, V.; MEARNS, L.; MENÉNDEZ, C.; RÄISÄNEN, J.; RINKE, A.; SARR, A. and WHETTON, P. (2007): Regional climate projections. In: SOLOMON, S.; QIN, D.; MANNING, M.; CHEN, Z.; MARQUIS, M.; AVERYT, K. B.; TIGNOR, M. and MILLER, H. L. (eds.): Climate change 2007: the physical science basis. Contribution of Working Group I to the Fourth Assessment Report of the Intergovernmental Panel on Climate Change. Cambridge, UK and New York, NY, USA.

FU, G.; GUO, J.; XIE, S.; DUAN, Y. and ZHANG, M. (2006): Analysis and high-resolution modeling of a dense sea fog event over the Yellow Sea. In: Atmospheric Research 81 (4), 293–303. DOI: 10.1016/j.atmosres.2006.01.005

GULTEPE, I.; MULLER, M. D. and BOYBEYI, Z. (2006): A new visibility parameterization for warm-fog applications in numerical weather prediction models. In: Journal of Applied Meteorology and Climatology 45 (11), 1469–1480. DOI: 10.1175/JAM2423.1

GULTEPE, I.; TARDIF, R.; MICHAELIDES, S. C.; CERMAK, J.; BOTT, A.; BENDIX, J.; MULLER, M. D.; PAGOWSKI, M.; HANSEN, B.; ELLROD, G.; JACOBS, W.; TOTH, G. and COBER, S. G. (2007): Fog research: a review of past achievements and future perspectives. In: Pure and Applied Geophysics 164 (6-7), 1121–1159. DOI: 10.1007/s00024-007-0211-x

HACHFELD, B. (2000): Rain, fog and species richness in the Central Namib Desert in the exceptional rainy season of 1999/2000. In: Dinteria 26, 113–146.

HACHFELD, B. and JUERGENS, N. (2000): Climate patterns and their impact on the vegetation in a fog driven desert: the Central Namib Desert in Namibia. In: Phytocoenologia 30 (3-4), 567–589.

HAEFFELIN, M; BERGOT, T.; ELIAS, T.; TARDIF, R.; CARRER, D.; CHAZETTE, P.; COLOMB, M.; DROBINSKI, P.; DUPONT, E.; DUPONT, J-C.; GOMES, L.; MUSSON-GENON, L.; PIETRAS,C.; PLANA-FATTORI, A.;PROTAT, A.; RANGOGNIO, J., RAUT, J-C.; RÉMY, S.; RICHARD, D.; SCIARE, J. and ZHANG, X. (2010): PARISFOG: shedding new light on fog physical processes. In: Bulletin of the American Meteorological Society 91 (6), 767–783.

HAENSLER, A.; HAGEMANN, S. and JACOB, D. (2010a): Regional climatological patterns and their simulated change. In: SCHMIEDEL, U. and JÜRGENS, N. (eds.): Biodiversity in southern Africa. Vol. 2: Patterns and processes at regional scale. Göttingen, Windhoek, 24–28.

– (2010b): Dynamical downscaling of ERA40 reanalysis data over southern Africa: added value in the representation of seasonal rainfall characteristics. In: International Journal of Climatology. DOI: 10.1002/joc.2242

– (2010c): How the future climate of the southern African region might look like: Results of a high-resolution regional climate change projection. In: Nova Acta Leopoldina, 112 (384), 183–193.

– (2011): The role of the simulation setup in a long-term high-resolution climate change projection for the southern African region. In: Theoretical and Applied Climatology. DOI: 10.1007/s00704-011-0420-1

HAMILTON, W. J.; HENSCHEL, J. R. and SEELY, M. K. (2003): Fog collection by Namib Desert Beetles. In: South African Journal of Science 99 (3-4), 181–181.

HENSCHEL, J. R. and SEELY, M. K. (2008): Ecophysiology of atmospheric moisture in the Namib Desert. In: Atmospheric Research 87 (3-4), 362–368. DOI: 10.1016/j.atmosres.2007.11.015

JACOB, D. (2001): A note to the simulation of the annual and inter-annual variability of the water budget over the Baltic Sea drainage basin. In: Meteorology and Atmospheric Physics 77, 61–73. DOI: 10.1007/s007030170017

Jᴀᴄᴏʙ, D. and Pᴏᴅᴢᴜɴ, R. (1997): Sensitivity studies with the regional climate model REMO. In: Meteorology and Atmospheric Physics 63 (1-2), 119–129. DOI: 10.1007/BF01025368

Jᴜɴɢᴄʟᴀᴜs, J.; Kᴇᴇɴʟʏsɪᴅᴇ, N.; Bᴏᴛᴢᴇᴛ, M.; Hᴀᴀᴋ, H.; Lᴜᴏ, J.; Lᴀᴛɪꜰ, M.; Mᴀʀᴏᴛᴢᴋᴇ, J.; Mɪᴋᴏʟᴀᴊᴇᴡɪᴄᴢ, U. and Rᴏᴇᴄᴋɴᴇʀ, E. (2006): Ocean circulation and tropical variability in the coupled model ECHAM5/MPI-OM. In: Journal of Climate 19 (16), 3952–3972. DOI: 10.1175/JCLI3827.1

Kᴜɴᴋᴇʟ, B. A. (1984): Parameterization of droplet terminal velocity and extinction coefficient in fog models. In: Journal of Climate and Applied Meteorology 23 (1), 34–41. DOI: 10.1175/1520-0450(1984)023<0034:PODTVA>2.0.CO;2

Lᴀɴᴄᴀsᴛᴇʀ, J.; Lᴀɴᴄᴀsᴛᴇʀ, N. and Sᴇᴇʟʏ, M. (1984): Climate of the central Namib Desert. In: MADOQUA 14 (1), 5–61.

Lᴏᴜɪs, J.-F. (1979): A parametric model of vertical eddy fluxes in the atmosphere. In: Boundary-Layer Meteorology 17, 187–202. DOI: 10.1007/BF00117978

MᴀᴄKᴇʟʟᴀʀ, N.; Hᴇᴡɪᴛsᴏɴ, B. and Tᴀᴅʀᴏss, M. (2007): Namaqualands climate: recent historical changes and future scenarios. In: Journal of Arid Environments 70 (4), 604–614. DOI: 10.1016/j.jaridenv.2006.03.024

Mᴀᴊᴇᴡsᴋɪ, D. (1991): The Europa-Modell of the Deutscher Wetterdienst. In: ECMWF Seminar on Numerical Methods in Atmospheric Models 2, 147–191.

Mᴜᴇʟʟᴇʀ, M. D.; Mᴀsʙᴏᴜ, M. and Bᴏᴛᴛ, A. (2010): Three dimensional fog forecasting in complex terrain. In: Quarterly Journal of the Royal Meteorological Society 136 (653), 2189–2202. DOI: 10.1002/qj.705

Nᴀᴋɪᴄᴇɴᴏᴠɪᴄ, N.; Aʟᴄᴀᴍᴏ, J.; Dᴀᴠɪs, G.; ᴅᴇ Vʀɪᴇs, B.; Fᴇɴʜᴀɴɴ, J.; Gᴀꜰꜰɪɴ, S.; Gʀᴇɢᴏʀʏ, K.; Gʀᴜʙʟᴇʀ, A.; Jᴜɴɢ, T.; Kʀᴀᴍ, T. and others (2000): Special report on emissions scenarios: a special report of Working Group III of the Intergovernmental Panel on Climate Change. Technical report, Pacific Northwest National Laboratory, Richland, WA (US). Environmental Molecular Sciences Laboratory (US).

Oʟɪᴠɪᴇʀ, J. (1995): Spatial distribution of fog in the Namib. In: Journal of Arid Environments 29 (2), 129–138. DOI: 10.1016/S0140-1963(05)80084-9

– (2004): Fog harvesting: an alternative source of water supply on the West Coast of South Africa. In: GeoJournal 61 (2), 203–214. DOI: 10.1007/s10708-004-2889-y

Oʟɪᴠɪᴇʀ, J. and ᴅᴇ Rᴀᴜᴛᴇɴʙᴀᴄʜ, C. J. (2002): The implementation of fog water collection systems in South Africa. In: Atmospheric Research 64 (1-4), 227–238. DOI: 10.1016/S0169-8095(02)00094-7

Oʟɪᴠɪᴇʀ, J. and Sᴛᴏᴄᴋᴛᴏɴ, P. L. (1989): The influence of upwelling extent upon fog incidence at Luderitz, Southern-Africa. In: International Journal of Climatology 9 (1), 69–75. DOI: 10.1002/joc.3370090106

Pᴀɢᴏᴡsᴋɪ, M.; Gᴜʟᴛᴇᴘᴇ, I. and Kɪɴɢ, P. (2004): Analysis and modeling of an extremely dense fog event in southern Ontario. In: Journal of Applied Meteorology 43 (1), 3–16. DOI: 10.1175/1520-0450(2004)043<0003:AAMOAE>2.0.CO;2

Pɪᴄᴋꜰᴏʀᴅ, M. and Sᴇɴᴜᴛ, B. (1999): Geology and palaeobiology of the Namib Desert, southwestern Africa. In: Geological Survey of Namibia Memoir 18.

Rᴏᴇᴄᴋɴᴇʀ, E.; Aʀᴘᴇ, K.; Bᴇɴɢᴛssᴏɴ, M.; Cʜʀɪsᴛᴏᴘʜ, M.; Cʟᴀᴜssᴇɴ, M.; Dᴜᴇᴍᴇɴɪʟ, L.; Esᴄʜ, M.; Gɪᴏʀɢᴇᴛᴛᴀ, M.; Sᴄʜʟᴇsᴇ, U. and Sᴄʜᴜʟᴢᴡᴇɪᴅᴀ, U. (1996): The atmospheric general circulation model ECHAM-4: model description and simulation of present-day climate. Max Planck Institute for Meteorology Report 218. Hamburg.

Rᴏᴇᴄᴋɴᴇʀ, E.; Bäᴜᴍʟ, G.; Bᴏɴᴀᴠᴇɴᴛᴜʀᴀ, L.; Bʀᴏᴋᴏᴘꜰ, R.; Esᴄʜ, M.; Gɪᴏʀɢᴇᴛᴛᴀ, M.; Hᴀɢᴇᴍᴀɴɴ, S.; Kɪʀᴄʜɴᴇʀ, I.; Kᴏʀɴʙʟᴜᴇʜ, L.; Mᴀɴᴢɪɴɪ, E.; Rʜᴏᴅɪɴ, A.; Sᴄʜʟᴇsᴇ, U.; Sᴄʜᴜʟᴢᴡᴇɪᴅᴀ, U. and Tᴏᴍᴘᴋɪɴs, A. (2003): The atmospheric general circulation model ECHAM5. Part I: Model description, Max Planck Institute for Meteorology Report 349. Hamburg.

Sᴄʜᴜʟᴢᴇ, B. (1969): The climate of Gobabeb. In: Scientific Papers of the Namib Desert Research Station 38, 5–12.

Sʜᴀɴɴᴏɴ, L. (1985): The Benguela ecosystem: 1. Evolution of the Benguela, physical features and processes. In: Oceanography and Marine Biology: An Annual Review 23.

Sʜᴀɴʏᴇɴɢᴀɴᴀ, E. S.; Hᴇɴsᴄʜᴇʟ, J. R.; Sᴇᴇʟʏ, M. K. and Sᴀɴᴅᴇʀsᴏɴ, R. D. (2002): Exploring fog as a supplementary water source in Namibia. In: Atmospheric Research 64 (1-4), 251–259. DOI: 10.1016/S0169-8095(02)00096-0

Sʜɪ, C.; Yᴀɴɢ, J.; Qɪᴜ, M.; Zʜᴀɴɢ, H.; Zʜᴀɴɢ, S. and Lɪ, Z. (2010): Analysis of an extremely dense regional fog event in Eastern China using a mesoscale model. In: Atmospheric Research 95 (4), 428–440. DOI: 10.1016/j.atmosres.2009.11.006

Sᴜɴᴅǫᴠɪsᴛ, H. (1978): A parameterization scheme for non-convective condensation including precipitation including prediction of cloud water content. In: Quarterly Journal of the Royal Meteorological Society 104, 677–690. DOI: 10.1002/qj.49710444110

Tᴀʀᴅɪꜰ, R. (2007): The impact of vertical resolution in the explicit numerical forecasting of radiation fog: a case study. In: Pure and Applied Geophysics 164 (6-7), 1221–1240. DOI: 10.1007/s00024-007-0216-5

Tᴇɪxᴇɪʀᴀ, J. (1999): Simulation of fog with the ECMWF prognostic cloud scheme. In: Quarterly Journal of the Royal Meteorological Society 125 (554), 529–552. DOI: 10.1002/qj.49712555409

Uᴘᴘᴀʟᴀ, S. M.; Käʟʟʙᴇʀɢ, P. W.; Sɪᴍᴍᴏɴs, A. J.; Aɴᴅʀᴀᴇ, U.; ᴅᴀ Cᴏsᴛᴀ Bᴇᴄʜᴛᴏʟᴅ, V.; Fɪᴏʀɪɴᴏ, M.; Gɪʙsᴏɴ, J. K.; Hᴀsᴇʟᴇʀ, J.; Hᴇʀɴᴀɴᴅᴇᴢ, A.; Kᴇʟʟʏ, G. A.; Lɪ, X.; Oɴᴏɢɪ, K.; Sᴀᴀʀɪɴᴇɴ, S.; Sᴏᴋᴋᴀ, N.; Aʟʟᴀɴ, R. P.; Aɴᴅᴇʀs-

son, E.; Arpe, K.; Balmaseda, M. A.; Beljaars, A. C. M.; van de Berg, L.; Bidlot, J.; Bormann, N.; Caires, S.; Chevallier, F.; Dethof, A.; Dragosavac, M.; Fisher, M.; Fuentes, M.; Hagemann, S.; Hólm, E.; Hoskins, B. J.; Isaksen, L.; Janssen, P. A. E. M.; Jenne, R.; McNally, A. P.; Mahfouf, J. F.; Morcrette, J. J.; Rayner, N. A.; Saunders, R. W.; Simon, P.; Sterl, A.; Trenberth, K. E.; Untch, A.; Vasiljevic, D.; Viterbo, P. and Woollen, J. (2005): The ERA-40 re-analysis. In: Quarterly Journal of the Royal Meteorological Society 131 (612), 2961–3012. DOI: 10.1256/qj.04.176

van der Velde, I.; Steeneveld, G.; Wichers Schreur, B. and Holtslag, A. (2010): Modeling and forecasting the onset and duration of severe radiation fog under frost conditions. In: Monthly Weather Review 138, 4237–4253. DOI: 10.1175/2010MWR3427.1

WMO (WORLD METEOROLOGICAL ORGANIZATION) (1992): International Meteorological Vocabulary. WMO Publications182. Geneva.

Zhou, B. B. and Du, J. (2010): Fog prediction from a multimodel mesoscale ensemble prediction system. In: Weather And Forecasting 25 (1), 303–322. DOI: 10.1175/2009WAF2222289.1

Authors

Dr. Andreas Haensler*
Dr. Stefan Hagemann
Prof. Dr. Daniela Jacob*
Max Planck Institute for Meteorology
Bundesstr. 53
D-20146 Hamburg
Germany

*now at the
Helmholtz-Zentrum Geesthacht
Climate Service Center (CSC)
Fischertwiete 1,
20095 Hamburg
Germany
andreas.haensler@hzg.de

Dr. Jan Cermak
Institute for Atmospheric and Climate Science,
ETH Zurich
Universitätstrasse 16
8092 Zürich
Switzerland
jan.cermak@env.ethz.ch